Calculation of the Maxwell stress tensor and the Poisson-Boltzmann force on a solvated molecular surface using hypersingular boundary integrals

Benzhuo Lu[a)]
Department of Chemistry and Biochemistry, Center for Theoretical Biological Physics, University of California at San Diego, La Jolla, California 92093-0365

Xiaolin Cheng
Center for Theoretical Biological Physics, Howard Hughes Medical Institute, University of California at San Diego, La Jolla, California 92093-0365

Tingjun Hou
Department of Chemistry and Biochemistry, Center for Theoretical Biological Physics, University of California at San Diego, La Jolla, California 92093-0365

J. Andrew McCammon
Department of Chemistry and Biochemistry, Center for Theoretical Biological Physics, Department of Pharmacology, Howard Hughes Medical Institute, University of California at San Diego, La Jolla, California 92093-0365

(Received 13 May 2005; accepted 30 June 2005; published online 1 September 2005)

The electrostatic interaction among molecules solvated in ionic solution is governed by the Poisson-Boltzmann equation (PBE). Here the hypersingular integral technique is used in a boundary element method (BEM) for the three-dimensional (3D) linear PBE to calculate the Maxwell stress tensor on the solvated molecular surface, and then the PB forces and torques can be obtained from the stress tensor. Compared with the variational method (also in a BEM frame) that we proposed recently, this method provides an even more efficient way to calculate the full intermolecular electrostatic interaction force, especially for macromolecular systems. Thus, it may be more suitable for the application of Brownian dynamics methods to study the dynamics of protein/protein docking as well as the assembly of large 3D architectures involving many diffusing subunits. The method has been tested on two simple cases to demonstrate its reliability and efficiency, and also compared with our previous variational method used in BEM. © *2005 American Institute of Physics*.
[DOI: 10.1063/1.2008252]

I. INTRODUCTION

The electrostatic interactions among biomolecules in ionic solution can be described by the Poisson-Boltzmann equation (PBE). Different methods have been developed to solve the PBE, such as finite difference (FD) methods,[1–3] finite element (FE) methods,[4,5] and boundary element methods (BEMs).[6,7] However, most of these works and their applications in biomolecular studies are focused on the electrostatic potential and interaction energy calculations. Relatively few studies have considered electrostatic force calculations. Dynamical study of biomolecular systems is of great interest in chemical physics and molecular biology. Therefore, the force calculation is important for many theoretical studies and molecular-dynamics (MD) simulations. PB forces have recently been applied in several MD simulations.[8–10] Gilson *et al.*[11] derived an expression for PB force calculation that is correct for the FD approach. The formula is compatible with the Maxwell stress tensor method, and a smooth dielectric boundary is required in that method. But for a system with two or more interacting macromolecules, as in protein assembly, the FD method is not practical for the full PB force calculation "on the fly" due to the tremendous CPU time required. The Brownian dynamics (BD) program in the UHBD (Ref. 12) actually uses a partial PB force between protein and ligand, because only the reaction field of the fixed protein is calculated. For rigid body problems, the BEM can use the molecular surface information repeatedly, so that it has fast performance for the full PB force updating required in a protein-protein encounter dynamics simulation. The force calculation in a BEM using a "polarized charge" method was first described by Zauhar;[13] the force included both qE forces and boundary pressures. This idea was used in a later BEM work.[8,14] In these works, the BEM used a single-layer representation. However, the accuracy of the boundary pressure computed by this technique has not yet been demonstrated. More generally, the use of only a single- or double-layer representation of the BEM to calculate the forces and torques has still not been adequately tested. In our recent work,[15] to our knowledge, we gave the first rigorous procedure for using a variational approach embedded in the BEM frame to calculate the full PB force and torque on a molecule in an interacting system with an arbitrary number of molecules in ionic solution. That is

[a)]Electronic mail: blu@mccammon.ucsd.edu

 © 2005 American Institute of Physics

Downloaded 20 Apr 2007 to 132.239.68.158. Redistribution subject to AIP license or copyright, see http://jcp.aip.org/jcp/copyright.jsp

based on the direct BEM solution (with both single-layer and double-layer terms). In the variational method, in order to obtain the PB force on a molecule, additional computations are needed to calculate matrices of coefficients linking the nodes on the discretized surface of the target molecule and those of the other molecules, to perform the matrix iterations, and finally to calculate the integral on the surface of every interacting molecule. Therefore, this is not efficient enough for macromolecular systems that have many nodes on the discretized surface(s). On the other hand, in theory, the PB force and torque on a molecule can be computed by integrating the stress tensor including the Maxwell stress tensor and the osmotic pressure of ions over its surface, and the stress tensor can be calculated directly from the BEM solution of the PBE. The PB force calculation after obtaining the BEM solution is then only related to the corresponding molecule, which is different from the variational approach, and this single integration per molecule can increase the force computation speed.

The Maxwell stress tensor depends on the electrostatic field, i.e., the negative gradient of the potential. A direct calculation of the gradient of the potential on the molecular surface will be subject to the so-called hypersingularity problem, which comes from the integration of the derivative of the Green's function associated with the double-layer part in the BEM. Fortunately, the hypersingular integral technique has been developed recently.[16,17] In this work, we use the hypersingular integral technique in a BEM for the three-dimensional (3D) linear PBE to calculate the derivatives of the potential at any position on a molecular surface, and consequently compute the total PB force and torque acting on the molecule in an interacting molecular system solvated in ionic solution. The increased efficiency makes it feasible to calculate the full PB force when applying BD simulation to study protein encounter or protein-protein docking. Another advantage of the present hypersingular integral method relative to the variational approach is that it gives the detail of the electrostatic stress everywhere on the surface, which facilitates the analysis of other related properties of the biomolecule. For example, the PB force can be partitioned to each surface atom, thus enabling all-atom BEMPB MD simulation. Our previous variational method only gives the total interaction PB force on a molecule.

The hypersingular integral algorithm is tested on a two-sphere system, each containing a point charge or a dipole in the sphere center. The results are compared with that from our previous method and the analytical ones.

II. BOUNDARY INTEGRAL EQUATION SOLUTION FOR THE POTENTIAL

For brevity, the electrostatic potential $\phi(x_p)$ is written as ϕ_p, where p is any position inside, outside, or on the boundary of the molecule. The linear PBE for an isolated molecule surrounded by an infinite homogeneous ionic solution can be written as

$$\nabla^2\phi_p^{\text{int}} = -\frac{1}{D_{\text{int}}}\sum_k q_k\delta(r_p - r_k), \quad p \in \Omega, \tag{1}$$

$$\nabla^2\phi_p^{\text{ext}} = \kappa^2\phi^{\text{ext}}(r_p), \quad p \in \bar{\Omega}, \tag{2}$$

where ϕ_p^{int} is the potential at position p inside the molecular domain $\Omega, S=\partial\Omega$ is its boundary, i.e., solvent-accessible surface, ϕ_p^{ext} is the potential at position p outside domain Ω, D_{int} is the interior dielectric constant, r_k is the position of the kth source point charge q_k of the molecule, and κ is the reciprocal of the Debye-Hückel screening length, which is is determined by the ionic strength of the solution. An integral form of the potential solutions for Eqs. (1) and (2) can be expressed as

$$\phi_p^{\text{int}} = \oint_S \left[G_{pt}\frac{\partial\phi_t^{\text{int}}}{\partial n} - \frac{\partial G_{pt}}{\partial n}\phi_t^{\text{int}}\right] dS_t + \frac{1}{D_{\text{int}}}\sum_k q_k G_{pk}, \quad p,k \in \Omega, \tag{3}$$

$$\phi_p^{\text{ext}} = \oint_S \left[-u_{pt}\frac{\partial\phi_t^{\text{ext}}}{\partial n} + \frac{\partial u_{pt}}{\partial n}\phi_t^{\text{ext}}\right] dS_t, \quad p \in \bar{\Omega}, \tag{4}$$

where n is the outward normal vector, and t is an arbitrary point on the boundary. G and u are the fundamental solutions of Eqs. (1) and (2), respectively,

$$G_{pq} = \frac{1}{4\pi r_{pq}}, \tag{5}$$

$$u_{pq} = \exp(-\kappa r_{pq})/4\pi r_{pq}. \tag{6}$$

When point p approaches surface S, it becomes

$$\frac{1}{2}\phi_p^{\text{int}} = \oint_S^{\text{PV}} \left[G_{pt}\frac{\partial\phi_t^{\text{int}}}{\partial n} - \frac{\partial G_{pt}}{\partial n}\phi_t^{\text{int}}\right] dS_t + \frac{1}{D_{\text{int}}}\sum_k q_k G_{pk}, \quad p \in S, \tag{7}$$

$$\frac{1}{2}\phi_p^{\text{ext}} = \oint_S^{\text{PV}} \left[-u_{pt}\frac{\partial\phi_t^{\text{ext}}}{\partial n} + \frac{\partial u_{pt}}{\partial n}\phi_t^{\text{ext}}\right] dS_t, \quad p \in S, \tag{8}$$

where PV denotes the principal value integral to avoid the singular point when $t \to p$ in the integral equations. In our former work,[15] we described a procedure using the BEM to solve this PBE, and extended it to an interacting system with an arbitrary number of molecules.

III. HYPERSINGULAR BOUNDARY INTEGRAL FOR FORCE CALCULATION

In an ionic solution, the full stress tensor on the boundary should include an additional term accounting for the ionic pressure besides the conventional Maxwell stress tensor.[11] It is

$$T_{ij} = D_{\text{ext}}E_iE_j - \frac{1}{2}D_{\text{ext}}E^2\delta_{ij} - \frac{1}{2}D_{\text{ext}}\kappa^2\phi^2\delta_{ij}, \tag{9}$$

where D_{ext} is the exterior dielectric constant, E is the electrostatic field, and δ_{ij} is the Kronecker delta function. The first two terms form the Maxwell stress tensor (the electric stress), and the last term represents the contribution of the

Downloaded 20 Apr 2007 to 132.239.68.158. Redistribution subject to AIP license or copyright, see http://jcp.aip.org/jcp/copyright.jsp

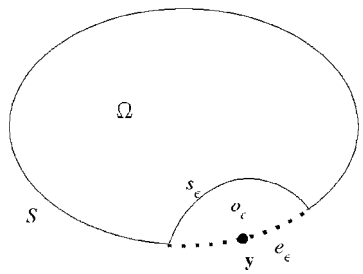

FIG. 1. Exclusion of the singular point y by a vanishing neighborhood o_ε. e_ε denotes the dotted part of the boundary.

osmotic pressure of ion to the stresses at the level of linear PBE. This term is considered to be part of the hydrodynamic stress rather than the electric stress. For a system with no convective flow (as is the case in this work), the above-mentioned formula gives the total stress present. Therefore, to obtain the boundary stress tensor, the derivative of the potential, that is, the negative of E on the boundary, should be known. In the integral form of the potential solution, Eqs. (3) and (4), the derivative of the potential with respect to position p, noted as $\phi_{,p}$, is obtained directly by differentiating on both sides of the equations, and then this value on the surface can be obtained by taking the limit as p approaches the boundary S. In order to use some results from the literature in which Laplace's equation is usually studied, here we first treat the interior potential solution of the PBE by subtracting the contribution of the source point charges of the molecule, that is

$$\nu_p = \phi_p^{\text{int}} - \frac{1}{D_{\text{int}}}\sum_k q_k G_{pk}, \quad p,k \in \Omega. \tag{10}$$

Then, the modified potential ν_p satisfies Laplace's equation, which is equal to the case without point charges. We will first calculate the derivative of ν_p, noted as $\nu_{,p}$, then return to the derivative of the original potential, i.e., $\phi_{,p}$, by recovering the contribution from the source point charges, which is easily calculated using Coulomb's law.

Now let us first consider the standard boundary integral equation for the harmonic function ν on the 3D domain Ω, bounded by the regular surface S (see Fig. 1),[16,18]

$$\lim_{\varepsilon\to 0^+}\int_{(S-e_\varepsilon)+s_\varepsilon}\left[\frac{\partial G(y,x)}{\partial n}\nu(x) - G(y,x)\frac{\partial \nu(x)}{\partial n}\right]dS(x) = 0. \tag{11}$$

The fundamental solution G has a weak singularity of order r^{-1}, when $r=|x-y|\to 0$, while its normal derivative has a strong singularity of order r^{-2}. Since in Eq. (11) both the points y and x lie on the surface S, a limiting process is necessary. Actually, since Eq. (11) stems from Green's second identity, it may be only formulated on a domain not including the singular point y. The situation is exemplified in Fig. 1, where a (vanishing) neighborhood o_ε of y has been removed from the original domain Ω. The integration is thus performed on the boundary $S_\varepsilon=(S-e_\varepsilon)+s_\varepsilon$ of the new domain $\Omega_\varepsilon=\Omega-o_\varepsilon$ (Fig. 1).

Differentiating Eq. (11) with respect to any coordinate y_i, we obtain

$$\lim_{\varepsilon\to 0^+}\int_{(S-e_\varepsilon)+s_\varepsilon}\left[V_i(y,x)v(x) - W_i(y,x)\frac{\partial v}{\partial n}\right]dS(x) = 0, \tag{12}$$

where

$$W_i = \frac{\partial G}{\partial y_i} = \frac{1}{4\pi r^2}r_{,i}, \tag{13}$$

$$V_i = \frac{\partial G}{\partial x_k\,\partial y_i}n_k(x) = -\frac{1}{4\pi r^3}\left[3r_{,i}\frac{\partial r}{\partial n} - n_i\right], \tag{14}$$

where $r_{,i}=\partial r/\partial x_i=-\partial r/\partial y_i$, and n_i is the ith component of the normal vector n. As expected, the kernel W_i shows a *strong* singularity of order r^{-2}, while the kernel V_i is *hypersingular* of order r^{-3}, as $r\to 0$.

Through the limiting process analysis as in Refs. 16 and 19 the hypersingular boundary integral equation for our modified electrostatic potential v can be written in the following form:

$$c_{ik}(y)v_{,k}(y) + \lim_{\varepsilon\to 0^+}\left\{\int_{(S-e_\varepsilon)}\left[V_i(y,x)v(x) - W_i(y,x)\frac{\partial v(x)}{\partial n}\right]dS(x) + v(y)\frac{b_i(y)}{\varepsilon}\right\} = 0, \tag{15}$$

where c_{ik} and b_i are (bounded) coefficients that only depend upon the local geometry of S at y. If y is a smooth boundary point (and s_ε had a spherical shape), the coefficient c_{ik} simply reduces to $0.5\delta_{ik}$. This is then similar to Eq. (4.4.5) in Ref. 19. This is the value we take in our case, because we consider that our molecular boundary has been smoothed before discretization.

The derivative of the potential appears in Eq. (15), but there still is a limiting process to be treated. We rearrange the equation in the hypersingular integral form on a discretized boundary for v in our study as

$$\frac{1}{2}v_{,i}(y) = -v_{,i}^o - \lim_{\varepsilon\to 0^+}\left\{\int_{(s_e-e_\varepsilon)}V_i(y,x)\frac{\partial v(x)}{\partial n}dS(x) + v(y)\frac{b_i(y)}{\varepsilon}\right\} + \lim_{\varepsilon\to 0^+}\int_{(s_e-e_\varepsilon)}W_i(y,x)v(x)dS(x), \tag{16}$$

where s_e denotes the boundary element(s) involving the singular point y, and $v_{,i}^o$ denotes the value from integration in Eq. (15) on all other elements $S-s_e$, which can be obtained by regular numerical integration. The term in brackets in Eq. (16), defined in terms of a limit, is called the "Hadamard"[20] or "finite part" of the unregularized integral, which is the hypersingular integral part. Guiggiani *et al.*[16] presented a procedure using Laurent series expansion to treat the general form of hypersingular integral and finally transformed it into a sum of a double integral and a one-dimensional regular integral. Then the standard quadrature formulas can be used. The procedure was improved a little bit later and expressed in a more complete form,[17] which does not affect the formulas for our case. Similar results can be obtained by using other approaches (see the appendixes of Ref. 17). The strong

Downloaded 20 Apr 2007 to 132.239.68.158. Redistribution subject to AIP license or copyright, see http://jcp.aip.org/jcp/copyright.jsp

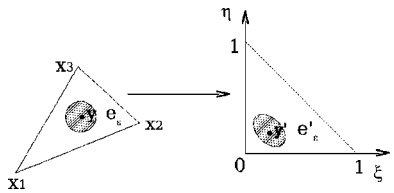

FIG. 2. A flat triangle in the three-dimensional space is mapped to a right isosceles triangle on the $\xi\eta$ plane. The singular point y, its surrounding circular patch e_ε, and their images in the transformed triangle are also shown.

singular integral part, i.e., the last term on the right-hand side of Eq. (16), can be treated following a similar procedure.

For our specific case, because we use a flat triangular element and linear shape functions, the derivation of hypersingular integral formulation can be more simple and straightforward. Here we give the detailed derivation. Let us first consider the case that the singular point y locates in the element, and suppose in the limiting process the patch e_ε is circular and of radius ε centered at point y (see Fig. 2). In this case, we can then show as following that part of the integral (the circular patch-related part) is solved analytically and the remainder numerically, which was also discussed by Allison.[21] In the implementation of the boundary element integral, the surface triangles in the physical three-dimensional space are mapped to an isosceles triangle on the $\xi\eta$ parametric plane, as shown in Fig. 2, where the integration on each element is actually performed.

The values of the coordinates, the potential, and its normal derivative at any position in the element are obtained by linear interpolation from the corresponding values on three nodes, respectively. For example, for a point (ξ,η) in parametric space, its coordinates in the original space is $x=N^1(\xi,\eta)x_1+N^2(\xi,\eta)x_2+N^3(\xi,\eta)x_3$, where N^i $(i=1,2,3)$ are the shape functions, and x_1,x_2,x_3 are the original coordinates of the three nodes of the element. Here, $N^1=(1-\xi-\eta)$, $N^2=\xi$, and $N^3=\eta$.

Now, we use polar coordinate (ρ,θ) in the parametric space (ξ,η) to perform the integral. Denoting Eq. (16) as

$$\frac{1}{2}v_{,i}=-v^o_{,i}-I+I^W, \tag{17}$$

we find that the hypersingular part I and the strong singular part I^W are

$$I=\lim_{\varepsilon\to 0^+}\left\{\int_{(s_e-e_\varepsilon)} V_i(y,x)N^\alpha v_n^\alpha J\rho d\rho d\theta+v(y)\frac{b_i(y)}{\varepsilon}\right\}, \tag{18}$$

$$I^W=\lim_{\varepsilon\to 0^+}\left\{\int_{(s_e-e_\varepsilon)} W_i(y,x)N^\alpha v^\alpha J\rho d\rho d\theta\right\}, \tag{19}$$

where v^α and v_n^α, $\alpha=1,2,3$, denote the value v and $\partial v(x)/\partial n$ at node α, respectively, and the doubly appeared superscripts (or subscripts) implicitly mean a summation, i.e., $N^\alpha v_n^\alpha=\Sigma_\alpha N^\alpha v_n^\alpha$. Note that $\partial r/\partial n=0$ on the flat surface, the hypersingular integrand in Eq. (18) is thus reduced to $(n_i/4\pi r^3)N^\alpha v_n^\alpha J\rho$, and the strong singular integral is given by $(r_i/4\pi r^2)N^\alpha v^\alpha J\rho$. J is the Jacobian from the coordinate transformation, and here simply doubles the element area,

From the coordinate transformation from r to (ξ,η), we find

$$x_i-y_i=\rho A_i(\theta), \tag{20}$$

$$r=\rho A(\theta), \tag{21}$$

where

$$A_i(\theta)=(x_2^i-x_1^i)\cos\theta+(x_3^i-x_1^i)\sin\theta, \tag{22}$$

$$A(\theta)=\left\{\sum_{i=1}^{3}[A_i(\theta)]^2\right\}^{1/2}, \tag{23}$$

and

$$N^\alpha=N_o^\alpha+\rho N_1^\alpha(\theta),\quad \alpha=1,2,3. \tag{24}$$

Here, A, A_i, N_0, and N_1 have the same definitions as in Ref. 16. N_0 is a constant that depends on the position of the singular point, namely, the position where we want to calculate the derivative of the potential. The contour of the neighborhood e_ε (given by the expression $\varepsilon=r$) now in the parameter plane is expressed in polar coordinates by

$$\varepsilon=\rho A_i(\theta). \tag{25}$$

By using the reversion of the above expression, we then obtain the expression in ε of the equation in polar coordinates of the contour e'_ε (the image of e_ε, see Fig. 2)

$$\rho=\varepsilon/A_i(\theta). \tag{26}$$

Now, using the above formulas (expansion) Eqs. (20)–(26) and performing the hypersingular and strong singular integrals, we obtain

$$I=\lim_{\varepsilon\to 0^+}\left\{\int_0^{2\pi}\left[\frac{A^{-3}Jn_iN_1^\alpha}{4\pi}(\ln|\hat\rho(\theta)|-\ln\varepsilon+\ln|A(\theta)|)-\frac{A^{-3}Jn_iN_0^\alpha}{4\pi}\left(\frac{1}{\hat\rho(\theta)}+\frac{1}{\varepsilon A(\theta)}\right)\right]d\theta+v(y)\frac{b_i(y)}{\varepsilon}\right\}, \tag{27}$$

$$I^W=\lim_{\varepsilon\to 0^+}\left\{\int_0^{2\pi}\left[\frac{A^{-3}A_iJN_1^\alpha}{4\pi}\hat\rho(\theta)+\frac{A^{-3}A_iJN_0^\alpha}{4\pi}(\ln|\hat\rho(\theta)|-\ln\varepsilon+\ln|A(\theta)|)\right]d\theta\right\}. \tag{28}$$

Note that $A(\theta)=A(\theta+\pi)$, $A_i(\theta)=-A_i(\theta+\pi)$, and $N_1^\alpha(\theta)=-N_1^\alpha(\theta+\pi)$, the integral of the terms involving $\ln\varepsilon$ in both Eqs. (27) and (28) is equal to zero. Because the final value I in Eq. (27) is finite, in the limiting process, the integral result of the term involving $1/\varepsilon$ must be canceled by the term $v(y)[b_i(y)/\varepsilon]$. Then, the singular integrals are transformed without any approximation into regular integrals (one dimension in our case), they are

$$I=\int_0^{2\pi}\left[F_{-1}(\theta)(\ln|\hat\rho(\theta)A(\theta)|)-F_{-2}(\theta)\frac{1}{\hat\rho(\theta)}\right]d\theta, \tag{29}$$

Downloaded 20 Apr 2007 to 132.239.68.158. Redistribution subject to AIP license or copyright, see http://jcp.aip.org/jcp/copyright.jsp

$$I^W = \int_0^{2\pi} [F_0^W(\theta)\hat{\rho}(\theta) + F_{-1}^W(\theta)(\ln|\hat{\rho}(\theta)A(\theta)|)]d\theta, \tag{30}$$

with

$$F_{-1}(\theta) = \frac{A^{-3}Jn_iN_1^\alpha}{4\pi}, \tag{31}$$

$$F_{-2}(\theta) = \frac{A^{-3}Jn_iN_0^\alpha}{4\pi}, \tag{32}$$

$$F_0^W(\theta) = \frac{A^{-3}A_iJN_1^\alpha}{4\pi}, \tag{33}$$

$$F_{-1}^W(\theta) = \frac{A^{-3}A_iJN_0^\alpha}{4\pi}. \tag{34}$$

The above two formulas hold for linear triangular boundary elements employed when the singular point is located in the element. A general form for hypersingular integral for any kind of boundary element employed can be found in Refs. 16 and 17. If the singular point is chosen to be nodal points on the bounding surface, a similar circular patch can be selected, but subdivided into parts belonging to different neighboring elements. Then a similar procedure presented above can be used, and the singular integral can be analytically resolved. The results become

$$I = \sum_m \left\{ \int_{\theta_1^m}^{\theta_2^m} \left[F_{-1}^m(\theta)(\ln|\hat{\rho}^m(\theta)A^m(\theta)|) - F_{-2}^m(\theta)\frac{1}{\hat{\rho}^m(\theta)} \right] d\theta \right\}, \tag{35}$$

$$I^W = \sum_m \left\{ \int_{\theta_1^m}^{\theta_2^m} [F_0^{Wm}(\theta)\hat{\rho}^m(\theta) + F_{-1}^{Wm}(\theta) \times (\ln|\hat{\rho}^m(\theta)A^m(\theta)|)]d\theta \right\}, \tag{36}$$

where the index m refers to the mth element around the collocation point, $F_{-1}^m(\theta)$, $F_{-2}^m(\theta)$, $F_{-1}^{Wm}(\theta)$, $F_0^{Wm}(\theta)$, and $A^m(\theta)$ are the similar coefficient as in Eqs. (29) and (30) but correspond to the mth element, and $\theta_1^m \leqslant \theta < \theta_2^m$ on the element. It should be noted here that, when the adjacent elements are on a plane, the sum of all the sectional angle ranges is equal to 2π. This was restated in the work of Huber *et al.*[22] However, in a real discretized surface such as the triangulated molecular surface in our case, the adjacent elements sharing a common node may deviate somewhat from a plane, and thus the sum of the angles might not be 2π. Nevertheless, in our present stress calculations on the node, we suppose that the molecular surface is smoothed enough and the adjacent elements around a node are nearly on a plane; Eqs. (35) and (36) are still used for the boundary integral on each related element. Because the integral on each element is also actually transformed onto an independent parametric triangle as is routinely done, the angle interval in the integral is $\pi/2$ if taking the singular node as the first node of each element in the transformation.

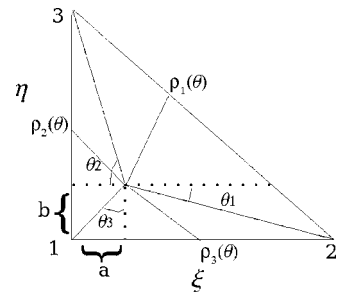

FIG. 3. A singular point in a parametric triangle.

In this work, we implement two options to select the collocation point, a singular point where the $v_{,i}$ is to be calculated. One is to select the point(s) in the element (not on the edge), which is(are) just the Gauss quadrature point(s) for the integration in Eqs. (29) and (30). We name this hypersingular integral method type I, denoted as HS1. The other option is to put the collocation point at each corner (node), and Eqs. (35) and (36) will be used, for which case the derivative of the potential at any point in the element will be obtained by interpolation. This second method is denoted as HS2.

For the first case where the singular point is selected as inside the triangular element, we just show the integral on the parametric triangle where the boundary element integral is actually performed. Figure 3 shows the singular point in a parametric triangle.

From the figure, the needed function $\hat{\rho}(\theta)$ can be calculated,

$$\hat{\rho}_1(\theta) = \frac{(1-a-b)\sin(\pi/4)}{\sin[(\pi/4)+\theta]}, \quad -\theta_1 \leqslant \theta < \pi - \theta_2,$$

$$\hat{\rho}_2(\theta) = \frac{a}{\cos(\pi-\theta)}, \quad \pi - \theta_2 \leqslant \theta < \frac{3}{2}\pi - \theta_3, \tag{37}$$

$$\hat{\rho}_3(\theta) = \frac{b}{\cos[\theta - (3/2)\pi]}, \quad \frac{3}{2}\pi - \theta_3 \leqslant \theta < 2\pi - \theta_1,$$

where $\theta_1 = \arctan b/(1-a)$, $\theta_2 = \arctan(1-b)/a$, $\theta_3 = \arctan a/b$, and (a,b) are the parametric coordinates of the singular point in the parametric triangle; e.g., if the singular point is in the center of the triangle, then $a=1/3$ and $b=1/3$.

The values in N in Eqs. (31)–(34) are

$$N_0^\alpha = \begin{cases} 1-a-b, & \alpha = 1 \\ a, & \alpha = 2 \\ b, & \alpha = 3, \end{cases}$$

and

$$N_1^\alpha(\theta) = \begin{cases} -\cos\theta - \sin\theta, & \alpha = 1 \\ \cos\theta, & \alpha = 2 \\ \sin\theta, & \alpha = 3. \end{cases} \tag{38}$$

Downloaded 20 Apr 2007 to 132.239.68.158. Redistribution subject to AIP license or copyright, see http://jcp.aip.org/jcp/copyright.jsp

In method HS2 for the singular point at the node of a triangular element, e.g., the first node (0,0), the functions in $\hat{\rho}(\theta)$ reduce to only one type,

$$\hat{\rho}(\theta) = \frac{1}{\cos\theta + \sin\theta}, \quad 0 \leqslant \theta < \frac{\pi}{2}, \tag{39}$$

and the functions in N are

$$N_0^\alpha = \begin{cases} 1, & \alpha = 1 \\ 0, & \alpha = 2 \\ 0, & \alpha = 3, \end{cases}$$

and

$$N_1^\alpha(\theta) = \begin{cases} -\cos\theta - \sin\theta, & \alpha = 1 \\ \cos\theta, & \alpha = 2 \\ \sin\theta, & \alpha = 3. \end{cases} \tag{40}$$

Now, all the essential elements are ready for the calculation of the derivatives of the potential on the molecular surface. The PB force calculation takes the following steps: First, we use the BEM to get the PBE solution (potentials and their normal derivatives) on the boundary elements for an arbitrary number of solvated molecules, as described in our former work.[15] Second, the singular integrals as described above are used to calculate the derivatives of the modified potential $v_{,i}$, then the derivatives of the potential $\phi_{,i}$ are obtained by adding the contribution of the source point charges to $v_{,i}$, and the stress tensor T at any point on the surface can be computed from Eq. (9). Finally, the PB force F and torque M acting on each molecule are calculated by integrations

$$F = \int_S T(x) \cdot dS(x), \tag{41}$$

$$M = \int_S r_c(x) \times [T(x) \cdot dS(x)], \tag{42}$$

where $r_c(x)$ is a vector from the center of mass of the target molecule to the surface point x, and the dot and cross vector multiplication are applied to the vector and tensor quantities.

IV. TESTS FOR SOME SIMPLE CASES

Since we have previously compared the potentials calculated from a variational approach with the analytical results on some cases,[15] here we just calculate and compare the electrostatic interaction forces between solvated molecules computed by all these methods. For a test model, we choose two point charges in vacuum, in which each charge is surrounded by a unit sphere discretized by 320 flat triangular elements (162 nodes). Both charges are put on the x axis, therefore, the nonzero force component is along the x direction, i.e., F_x, and the other two components F_y and F_z are zero in theory. Figure 4 shows the forces F_x along the x direction as a function of the distance between the two point charges calculated using the two hypersingular integral methods HS1 and HS2, the variational approach, and the analytical formula.

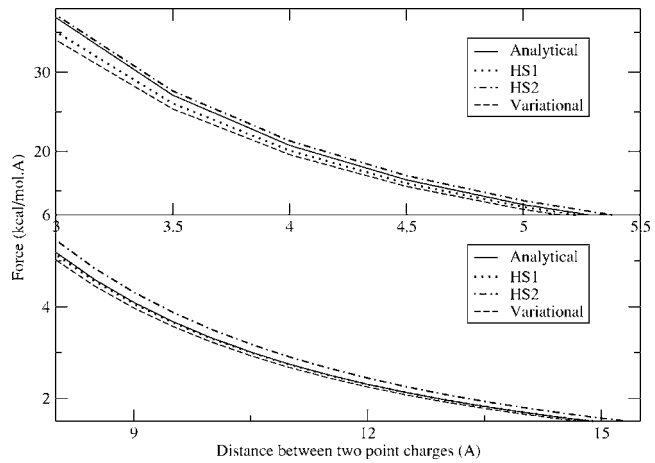

FIG. 4. The force calculation comparison using different approaches: analytical results (solid line), hypersingular integral type I (HS1) with singular point in the center of each element (dotted line), hypersingular integral type II (HS2) with singular point on the nodes (dot-dashed line), and variational approach (dashed line).

It is found that the forces F_x calculated by both HS1 and the variational approach are very close to the analytical ones in all the distance range shown in Fig. 4. The results from the hypersingular integral method HS1 are even more accurate than those from the variational approach; the HS1 curve is between those obtained by analytical solution and the variational approach over all the range. For HS2, the results at close distance are even more accurate than those from method HS1, but HS2 is less accurate at a large distance. It is also found that the more separated the two charges become, the smaller the relative errors of HS1 and the variational methods are. For example, the relative errors given by the variational approach and the HS1 method at a distance of 4 Å are 5.6% and 3.1%, respectively, and 2.8% and 0.3% at a distance of 10 Å, respectively. HS2 gives a more accurate result with a relative error of 2.7% at distance of 4 Å, but a bigger relative error (5.6%) at a distance of 10 Å. One reason may be the approximation of treating the adjacent elements as on a plane when using Eqs. (35) and (36), as mentioned above. Another possible reason will be discussed later. In addition, note that as mentioned in our previous work the force calculations at moderate to large distances are even more accurate than the potential itself on the boundary. This is quite promising for BD trajectory calculations.

It has to be noted that in our calculations the other two force components F_y and F_z that should be zero are very small (less than 10^{-5}) in the variational approach, while in hypersingular integral method HS1, these numbers are not as small, although they are still small relative to the nonzero component F_x (e.g., $F_y = 0.14$ kcal/mol Å and $F_z = 0.28$ kcal/mol Å at 4-Å distance). At larger distances, these two force components do not decrease much, thus the relative errors of these force components will be increased at a long distance. This is mostly due to the numerical error inherently existing in the algorithms. Comparing the two approaches (refer to previous work[15]), we find that the interaction between molecules calculated using the variational approach depends on $\Delta\phi$, which is the difference of the potential on the molecular surface in the interacting molecular

Downloaded 20 Apr 2007 to 132.239.68.158. Redistribution subject to AIP license or copyright, see http://jcp.aip.org/jcp/copyright.jsp

system relative to that in the isolated case. Therefore $\Delta\phi$, and consequently the force calculation, directly depend on the distance between the molecules. This keeps the relative accuracy more constant over almost all the distance ranges where the BEM is valid. But for the hypersingular integral method, as described in Sec. III the calculation of the derivative of the potential $v_{,i}$ depends on the total potential including $\Delta\phi$ due to the interaction, as well as the potential from the isolated molecule ϕ_{isol} that is fixed independent of the relative positions of the two molecules. Therefore, at a large distance, even if $\Delta\phi$ is small, ϕ_{isol} stays the same; the numerical error due to this part is maintained, and this makes the relative error increase. However, as illustrated by the above example, the relative error does not increase for the main force component, e.g., F_x. So, it seems that the relative errors of the variational approach are more stable and independent of the relative position of the molecules, while for molecules that are closer together, where the interaction is expected to be strong, the hypersingular methods give more accurate results.

An interesting thing is to check how much the singular integral parts (including strong and hypersingular) contribute to the total calculated electrostatic field. In the HS1 method, the singular integral contribution is just from the integration on one element where the singular point is located, and the other part is from the integral on all of the other elements. However, it is found that the singular integral contribution is large enough to offset the contributions from all the other elementary integrals. For example, at 4-Å distance in the above case, at the center of the first element, the singular integral part (HS1) gives the contributions to the electrostatic field −47.86, −34.84, and −347.17 kcal/mol Å e on x, y, and z directions, respectively, and the regular integral part gives 59.59, 36.55, and 364.69 kcal/mol Å e on x, y, and z directions, respectively. Therefore, the singular integral part cannot be omitted in the stress tensor calculation in the BEM.

The main advantage of the hypersingular integral method is its calculation efficiency, which is also the main motivation to develop this method, as mentioned above. In the above test case, in which 30 calculation points were selected as shown in Fig. 4, the CPU time on an Intel Pentium IV(2 GHz) for the whole BEM calculation is 28.3 s for the variational approach, 23.0 s for HS1, and 19.3 s for HS2. Moreover, as shown in the methods sections, the CPU time spent on the force calculation for the hypersingular integral is only dependent on the boundary elements on the target molecule, i.e., $\sim N_{\text{elem}}^2$, while that in the variational approach is dependent on all the boundary elements of the molecular systems. Therefore, for a large biomolecular system, the hypersingular integral methods should display much more efficiency than in the above simple system.

The second testing model is a point charge interacting with a dipole. The point charge surrounded by a unit spherical boundary is located at $(-2,0,0)$; the dipole is also surrounded by a unit spherical boundary with its two point charges located at (2, 0, 0.1) and $(2,0,-0.1)$, respectively. In this model, there are both force and torque acting on the dipole, but only the z direction force component F_z and the y direction torque component M_y are in principle not zero. The analytical solutions are $F_z^{\text{analy}}=-1.04$ kcal/mol Å, and $M_y^{\text{analy}}=-4.15$ kcal/mol. The variational approach gives $F_z=-1.02$ kcal/mol Å, and $M_y=-4.08$ kcal/mol, and the hypersingular integral method HS1 gives $F_z=-1.01$ kcal/mol Å, and $M_y=-4.01$ kcal/mol, and they are all close to the correct values. HS2 gives $F_z=-1.15$ kcal/mol Å, and $M_y=-4.58$ kcal/mol. The results of HS2 have a relatively large deviation from the analytical values, and show a less accuracy than HS1 again.

V. CONCLUSIONS AND DISCUSSION

We use the hypersingular integral technique in a BEM frame to directly calculate the derivatives of the potential on the molecular boundary, and then the Maxwell stress is obtained and used to compute the PB force on a molecule in an interacting solvated molecular system. The computational accuracy and performance for force and torque are demonstrated in the sample tests and compared with that of the previous variational approach. The accuracy of the hypersingular integral method (HS1) is found to be even somewhat higher than that of the variational method for the main force component computation. Compared with HS2, the first kind of hypersingular integral method (HS1) is rigorous in principle without the plane approximation for the adjacent boundary elements, and it has a stable computational performance in terms of accuracy in different cases. Overall, the major advantage of this hypersingular integral method is its faster performance compared with the variational approach, especially for biomolecular systems, and this makes it potentially useful for the BD simulation of protein-protein docking.

ACKNOWLEDGMENTS

This work was supported in part by the NIH, NSF, the Howard Hughes Medical Institute, National Biomedical Computing Resource, the NSF Center for Theoretical Biological Physics, SDSC, the W. M. Keck Foundation, and Accelrys, Inc.

[1] M. E. Davis and J. A. McCammon, J. Comput. Chem. **10**, 386 (1989).
[2] M. Holst, R. E. Kozack, F. Saied, and S. Subramaniam, J. Biomol. Struct. Dyn. **11**, 1437 (1994).
[3] A. Nicholls and B. Honig, J. Comput. Chem. **12**, 435 (1991).
[4] T. J. You and S. C. Harvey, J. Comput. Chem. **14**, 484 (1993).
[5] M. Holst, N. Baker, and F. Wang, J. Comput. Chem. **21**, 1319 (2000).
[6] R. J. Zauhar and R. S. Morgan, J. Mol. Biol. **186**, 815 (1985).
[7] H. X. Zhou, Biophys. J. **65**, 955 (1993).
[8] B. Z. Lu, C. X. Wang, W. Z. Chen, S. Z. Wan, and Y. Y. Shi, J. Phys. Chem. B **104**, 6877 (2000).
[9] B. Z. Lu, W. Z. Chen, C. X. Wang, and X. J. Xu, Proteins **48**, 497 (2002).
[10] R. Luo, L. David, and M. K. Gilson, J. Comput. Chem. **23**, 1244 (2002).
[11] M. K. Gilson, M. E. Davis, B. A. Luty, and J. A. McCammon, J. Phys. Chem. **97**, 3591 (1993).
[12] J. D. Madura, J. M. Briggs, R. C. Wade *et al.*, Comput. Phys. Commun. **91**, 57 (1995).
[13] R. J. Zauhar, J. Comput. Chem. **12**, 575 (1991).
[14] A. J. Bordner and G. A. Huber, J. Comput. Chem. **24**, 353 (2003).
[15] B. Z. Lu, D. Q. Zhang, and J. A. McCammon, J. Chem. Phys. **122**, 214102 (2005).
[16] M. Guiggiani, G. Krishnasamy, T. J. Rudolphi, and F. J. Rizzo, Trans. ASME, J. Appl. Mech. **59**, 604 (1992).
[17] M. Guiggiani, in *Singular Integrals in Boundary Element Methods*,

Downloaded 20 Apr 2007 to 132.239.68.158. Redistribution subject to AIP license or copyright, see http://jcp.aip.org/jcp/copyright.jsp

edited by V. Sladek and J. Sladek (Computational Mechanics, Southampton, UK, 1998), Chap. 3, pp. 85–124.
[18] O. D. Kellog, *Foundations of Potential Theory* (Frederick Ungar, New York, 1929).
[19] C. Pozrikidis, *A Practical Guide to Boundary-Element Methods with the Software Library BEMLIB* (Chapman and Hall, London, 2002).
[20] J. Hadamard, *Lectures on Cauchy's Problem in Linear Partial Differential Equations* (Dover, New York, 1952).
[21] S. A. Allison, Macromolecules **29**, 7391 (1996).
[22] O. Huber, A. Lang, and G. Kuhn, Comput. Mech. **12**, 39 (1993).

Downloaded 20 Apr 2007 to 132.239.68.158. Redistribution subject to AIP license or copyright, see http://jcp.aip.org/jcp/copyright.jsp